Chapter 31
Multi-objective Optimisation of Electro Jet Drilling Process Parameters for Machining of Crater in High-Speed Steel Using Grey Relational Analysis

Kalinga Simant Bal ⓘ**, Amal Madhavan Nair** ⓘ**, Dipanjan Dey** ⓘ**,
Anitesh Kumar Singh** ⓘ **and Asimava Roy Choudhury** ⓘ

Abstract In the present investigation, electro jet drilling has been implemented to machine crater in the high-speed steel sheet. Input parameters (applied voltage, electrolyte concentration, and standoff distance) were varied to study the change in output characteristics of the crater (mass removal rate (MRR), roundness error (RE) and mean diameter-to-height ratio (DHR)). MRR was found to increase with the increase in applied voltage and electrolyte concentration, while an increase in standoff distance was found to cause a decrease in MRR. RE was found to increase with applied voltage and standoff distance, while the increase in electrolyte concentration was found to cause a reduction in RE. DHR was increased with the increase in electrolyte concentration and standoff distance, while an increase in applied voltage resulted in the decrease of mean DHR. Optimization of input parameters was carried out to (a) maximize MRR and mean DHR and (b) minimize RE, of the machined crater, using Taguchi grey relation analysis.

Keywords Electro jet drilling · High-speed steel · Optimisation · Electrochemical machining · Crater

31.1 Introduction

Machining of micro- and macro-holes in hard-to-machine materials have gained prominence for use in aerospace, medical, electronic, computer, and optics industry. The need for machining accurate holes has led researchers looking into new nontraditional techniques. Electro jet drilling (EJD) is one such process that has the potential to meet the stringent demands of the industry offering significant advantages in accuracy, ease of material removal and micro-hole cutting ability. This process utilizes a

K. S. Bal · A. M. Nair · D. Dey · A. K. Singh · A. Roy Choudhury (✉)
Laser Material Processing Laboratory, Mechanical Engineering Department, Indian Institute of Technology Kharagpur, Kharagpur 721302, West Bengal, India
e-mail: archie@mech.iitkgp.ac.in

negatively charged stream of electrolyte which is allowed to impinge on the work-piece, and the material is removed via electrolytic dissolution. This eliminates the need for fabrication of micro-tools and tools that are harder than the material to be worked upon. Mohan and Shan [1, 2] generated small holes by electrochemical jet drilling process and studied the effects of different process parameters on the quality of the holes. Response surface methodology was applied to optimize the input process parameters and to enhance the output quality [1, 2]. Mohan and Shan [3, 4] used hybrid neural network, desirability function and genetic algorithm to optimize the process parameters of electrochemical drilling process. With the help of these multi-object optimization techniques, material removal rate and surface quality were enhanced significantly [3, 4]. Conductive mask electrochemical machining [5] was applied to reduce undercutting of micro-dimple and improve the machining localization. With the help of simulation, etch factor was improved significantly [5]. Liu et al. [6] carried out electrochemical jet machining on TB6 titanium alloy and studied the feasibility of the process. Optimum process parameters were found out to improve the output characteristics such as material removal rate and surface quality [6]. Hua and Xu [7] incorporated hybrid technology, i.e., laser drilling with electrochemical jet drilling, to remove the recast layer and spatter generated during the laser drilling. The output was improved significantly but the efficiency was reduced to 30%. Goel and Pandey [8] developed electrochemical jet drilling experimental setup and studied the effects of several inputs on different output characteristics like hole taper and material removal rate. They [8] successfully fabricated 140-micron diameter micro-hole with the help of their setup. Kozak et al. [9] developed a mathematical model on electrochemical jet machining process relating the machining rate with the working condition. The mathematical model was used to determine the maximum material removal rate and electrolyte flow for a fixed set of input process parameters. Ming et al. [10] studied kerosene submerged electrochemical jet drilling process and reported that the localization of the machining was possible by submerging both the workpiece and the nozzle. Endo et al. [11] machined small hole by electrochemical jet drilling process, and applied Fourier analysis to estimate the accuracy of the drilled hole. Natsu et al. [12] proposed a method to develop 3D surfaces with the help of micro electrolyte jet machining and discussed the possible way to find effective nozzle path and scan speed.

31.2 Problem Definition

Machining of crater using electrochemical drilling requires insulation of electrode tip at sides to prevent overcut caused due to the stray machining effect. Also, it is required for electrochemical drilling to immerse the sample completely in the electrolyte solution. This causes the development of electrode potential between the sample and the electrolyte, and could result in corrosion of the sample. Hence, electro jet drilling could be alternative to machine crater of suitable dimension, because (a) the crater dimension does not depend on the tool diameter, and at the same time (b)

sample is not completely immersed in the electrolyte solution. So, in the present study, machining of the crater has been carried out using electro jet drilling technique. For this purpose, nozzle diameter through which electrolyte jet impinges on the sample has been increased to facilitate the machining of the crater.

31.3   Experimental Details

High-speed steel sheet of dimension 30 mm × 10 mm × 1 mm was sectioned and polished in SiC abrasive paper to remove the surface contaminants. Table 31.1 shows the chemical composition of the high-speed steel sheet. After ultrasonic cleaning in 2-Propanol solution, the sample was clamped in the sample holder in the electro jet drilling machine. Figure 31.1 shows the electro jet drilling setup. A platinum wire having diameter of 0.5 was used as a tool. The platinum wire was recessed within the glass nozzle of outlet diameter of 0.75 mm. DC power supply was used in this experimentation. The tool was connected with the negative terminal of the power supply, and the high-speed steel substrate was connected with the positive terminal of the power supply. Electrolyte flow was supplied concentrically with the tool.

Table 31.1 Composition of the high-speed steel sheet used in the present study

Element	Fe	Cr	Mo	W	C	V
wt.%	82.15	3.98	5.01	6.11	0.77	1.98
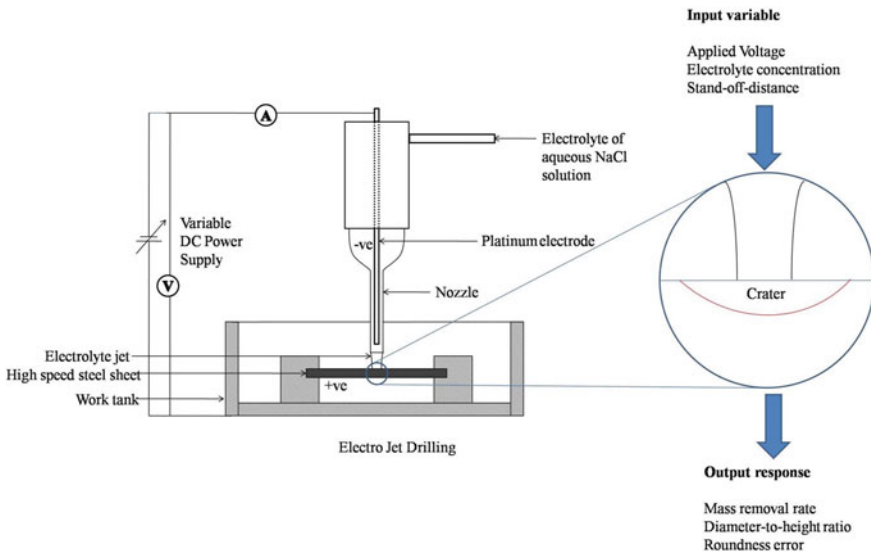
Fig. 31.1 Electro jet drilling setup

Table 31.2 Input process
parameters

Applied voltage (V)	Electrolyte concentration (N)	Standoff distance (mm)
20, 40, 60	0.1, 0.3, 0.5	0.5, 1.0, 1.5

750 W reciprocating type three-phase pump was used to supply the metered quantity of electrolyte solution into the required machining zone. NaCl aqueous solution with variable concentration was used as the electrolyte for machining.

Applied voltage, electrolyte concentration, and standoff distance were chosen as the input parameters. Table 31.2 shows the input process parameters along with their levels used in the experiment. Taguchi L9 orthogonal array was used to design the experimental run. Machining time for each run was 1 min. Output responses chosen for the present study include mass removal rate from the crater, roundness error and mean diameter-to-height ratio of the crater. The mass removal rate is defined as the weight loss of the sample per unit time after the machining. The roundness error of the crater is defined as the difference between the maximum crater diameter and the minimum crater diameter. The mean diameter-to-height ratio of the crater is defined as the ratio of the average diameter of the crater and the depth of the crater. In the present study, it is desired to increase the mass removal rate from the crater as well as increase the mean diameter-to-height ratio of the crater that would decrease the specific cutting energy (i.e., power required to remove a unit volume of material). Simultaneously, it is desired to reduce the roundness error of the crater to improve the circularity of the machined zone. Hence, grey relation analysis is used in the present study to solve the multi-objective optimization problem to obtain crater of the desired dimension.

31.4   Result and Discussion

Table 31.3 shows the output responses corresponding to the combination of input parameters designed according to Taguchi L9 run. The effect of input process parameters on output responses has been discussed in details below.

31.4.1   Effect of Process Parameters on Mass Removal Rate

Figure 31.2 shows the effect of process parameters on the mass removal rate of the high-speed steel sheet. It could be observed that the mass removal rate was found to increase with the increase in the applied voltage and the electrolyte concentration, while an increase in the standoff distance was found to cause a decrease in the mass removal rate. An increase in the applied voltage causes an increase in the current, and results in the increase in the mass removal rate. Figure 31.3 shows the increase in

Table 31.3 Output responses corresponding to the combination of input parameters according to Taguchi L9 run

Run	Input parameter			Output response		
	Applied voltage (V)	Electrolyte concentration (N)	Standoff distance (mm)	Avg. mass removal rate (mg/min)	Avg. roundness error (mm)	Avg. mean diameter-to-height ratio
1	20	0.1	0.5	3.81	0.246	20.3593
2	20	0.3	1.0	2.96	0.533	73.4251
3	20	0.5	1.5	1.23	0.2455	108.1178
4	40	0.1	1.0	4.34	0.346	36.4649
5	40	0.3	1.5	5.01	0.283	74.5380
6	40	0.5	0.5	5.22	0.3715	18.8301
7	60	0.1	1.5	2.25	0.857	56.9229
8	60	0.3	0.5	6.19	0.4295	18.0141
9	60	0.5	1.0	7.86	0.507	40.9559
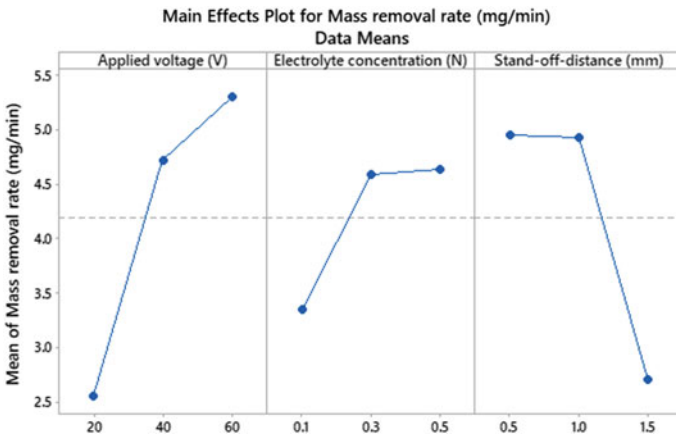
Fig. 31.2 Effect of process parameters on mass removal rate

the crater dimension with the applied voltage. The increase in NaCl concentration of the electrolyte solution causes an increase in the number of ions (Na$^+$ and Cl$^-$), and hence, the conductivity of the electrolyte solution increases. This result in the increase in the mass removal rate due to the increase in current flow in the solution. The increase in the standoff distance causes an increase in the flaring of the electrolyte jet. This causes a decrease in the effectiveness of the electrolyte jet column for carrying out machining, and hence, the mass removal rate decreases.
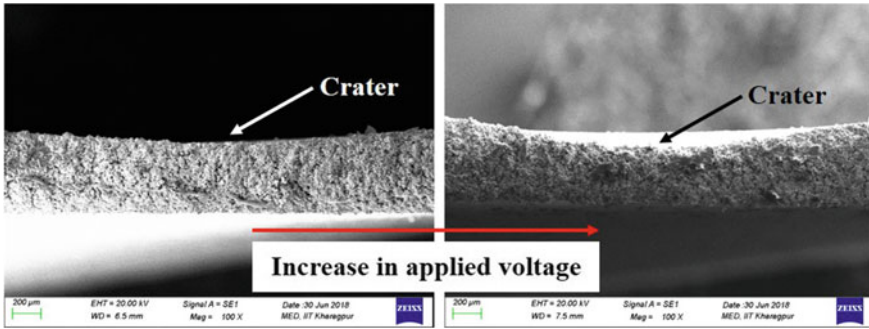
Fig. 31.3 Increase in crater dimension with applied voltage

31.4.2 Effect of Process Parameters on Roundness Error of Top of the Crater

Figure 31.4 shows the effect of process parameters on the roundness error of the top of the crater. It could be observed that the roundness error was found to increase with the increase in the applied voltage and the standoff distance, while an increase in electrolyte concentration was found to cause a decrease in the roundness error. Higher electrolyte concentration increases the ion availability in the solution, and might lead to homogeneous electrochemical dissolution. Consequently, higher electrolyte concentration could have lowered the roundness error. The conductivity of the electrolytic cell is inversely proportional to the standoff distance, and thus, inhomogeneous electrolytic dissolution could have occurred at high standoff distance. If the applied voltage exceeds the threshold voltage, then the spark may occur. Thus, at
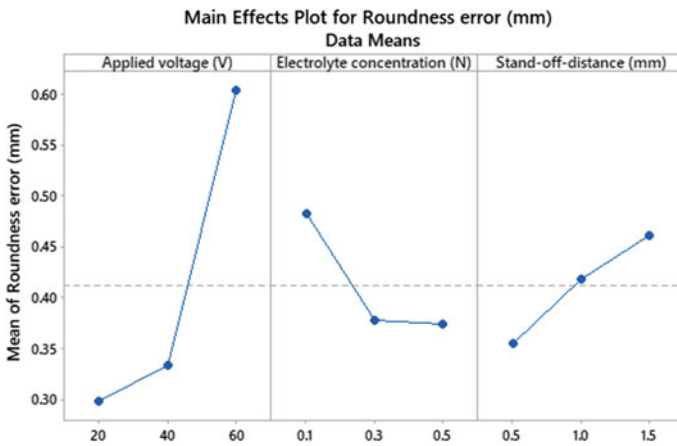

Fig. 31.4 Effect of process parameters on roundness error of top of the crater
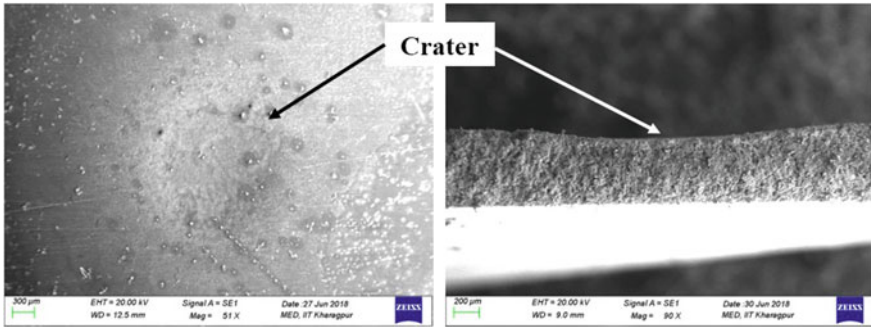
Fig. 31.5 Crater formation due to electro jet drilling

high applied voltage, spark occurring at the tool-workpiece interface might lead to higher roundness error. Figure 31.5 shows the crater formation due to the electro jet drilling.

31.4.3 Effect of Process Parameters on Mean Diameter-to-Height Ratio of the Crater

Figure 31.6 shows the effect of process parameters on the mean diameter-to-height ratio of the crater. It could be observed that the mean diameter-to-height ratio of the crater was found to increase with the increase in the electrolyte concentration and the standoff distance, while the increase in applied voltage was found to
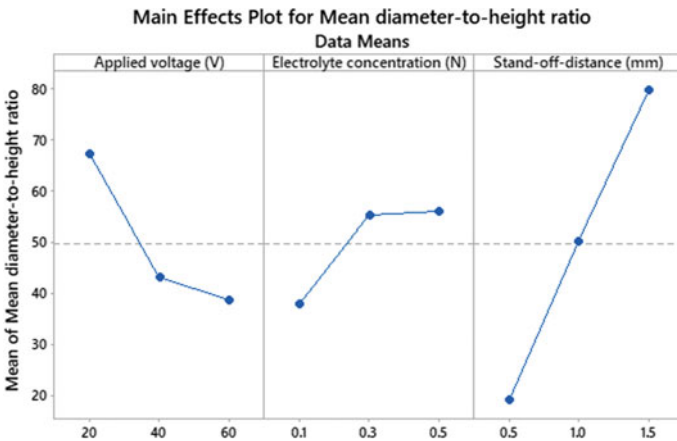

Fig. 31.6 Effect of process parameters on mean diameter-to-height ratio of the crater

cause a decrease in the mean diameter-to-height ratio. With the increase in stand-off distance, material dissolution becomes less, and height of the crater obtained is lower, and thus, the mean diameter-to-height ratio increases. Less material dissolution occurred at lower applied voltage, thus height of the crater is reduced. Consequently, diameter-to-height ratio is increased on decreasing the applied voltage. As NaCl is non-passivating electrolyte, thus increase in the concentration causes more dissolution because no oxide film formation occurs on the workpiece at the time of electrochemical reaction. So, with the increase in the electrolyte concentration, the diameter as well as the height of the crater increases. However, after the reaction, sludge ($FeCl_3$) produced is precipitated in the machining zone, and thus, it is difficult to replace the sludge completely by the fresh electrolyte in that intricate zone. So, machining along the depth became difficult, and thereby, on increasing the electrolyte concentration, the diameter of the crater is increased more as compare to the increment of the height of the crater. Hence, with the increase in electrolyte concentration, the mean diameter-to-height ratio is increased. The probable reaction [1] for the formation of $FeCl_3$ is as shown below:

Electrolytic reaction	Anodic reaction	Cathodic reaction
$NaCl \leftrightarrow Na^+ + Cl^-$ $H_2O \leftrightarrow H^+ + OH^-$ $Na^+ + OH^- \leftrightarrow NaOH$	$Fe \rightarrow Fe^{2+} + 2e^-$ $Fe^{2+} + 2Cl^- \rightarrow FeCl_2$ $FeCl_2 + Cl^- \rightarrow FeCl_3 \downarrow$	$2H^+ + 2e^- \rightarrow H_2 \uparrow$

31.4.4 Optimization of Process Parameters Using Grey Relational Analysis

In Fig. 31.7 grey relational grade for each experimental run has been shown. It is desired to maximize the mass removal rate and mean diameter-to-height ratio, and minimize the roundness error of the machined crater. So, considering the desired aspects for all the outputs, higher grey relational grade value results in better performance characteristics. Thus experiment number 9 has the highest value of grey relational grade among all the nine experimental runs as shown in Fig. 31.7. However, upon combining the input process parameters, there could be another set of input parameters that might show better performance than these nine runs. The average grey relational grade is determined to determine the best optimum process parameters.

In Fig. 31.8, the average grey relational grade for each level of process parameters has been shown. Among all the three level of each process parameters, the level that shows the highest average grey relational grade would be chosen as the best level for that process parameter. Thus, from the Fig. 31.8 it can be observed that the best combination of optimal set of input process parameters are: (a) applied voltage: level 3 (=60 V); (b) electrolyte concentration: level 3 (=0.5 N); and (c) standoff distance:
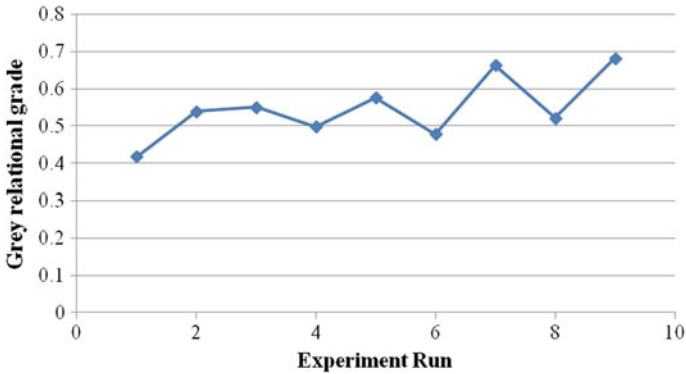
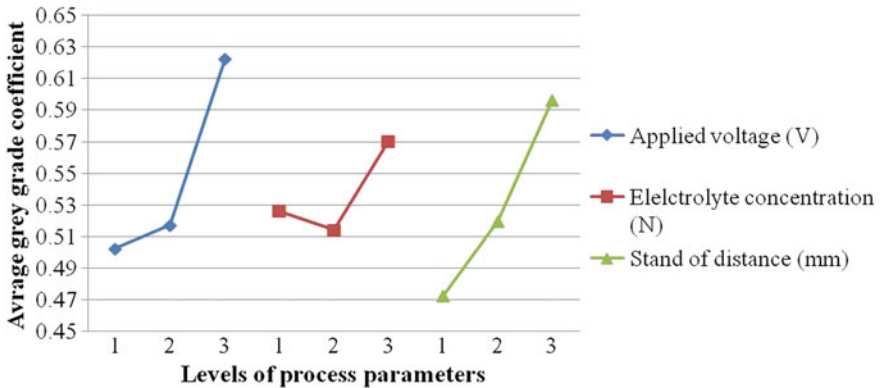**Fig. 31.7** Variation of grey relational grade with experimental run

**Fig. 31.8** Variation of average grey relational grade with the level of process parameter

level 3 (=1.5 mm). Hence, the analysis of the average value of grey relational grade shows that keeping the applied voltage (=60 V) and electrolyte concentration (=0.5 N) constant, an increase in standoff distance from 1.0 to 1.5 mm would result in a desired crater dimension. A confirmation experiment was performed using the optimal set of input process parameters obtained through the analysis of grey relational grade. Table 31.4 shows the comparison of output responses obtained using "experimental run 9" and "optimum combination of process parameters obtained through grey relational grade analysis". It was observed that the increase in the standoff distance from 1.0 mm to 1.5 mm resulted in the improvement of the average values of mass removal rate, roundness error and mean diameter-to-height ratio of the machined crater. Figure 31.9 shows the crater formed at the optimal combination of process parameters obtained through grey relational grade analysis.

In addition, the highest difference of average grey relational grade between the levels of each process parameters indicates the influence of that process parameters

Table 31.4 Output responses obtained using "experimental run 9" and "optimum combination of process parameters obtained through grey relational grade analysis"

Run	Input parameter			Output response		
	Applied voltage (V)	Electrolyte concentration (N)	Standoff distance (mm)	Avg. mass removal rate (mg/min)	Avg. round-ness error (mm)	Avg. mean diameter-to-height ratio
Run 9	60	0.5	1.0	7.86	0.50	40.95
Optimized	60	0.5	1.5	8.69	0.45	74.98

Fig. 31.9 Crater formed at the optimal combination of process parameters
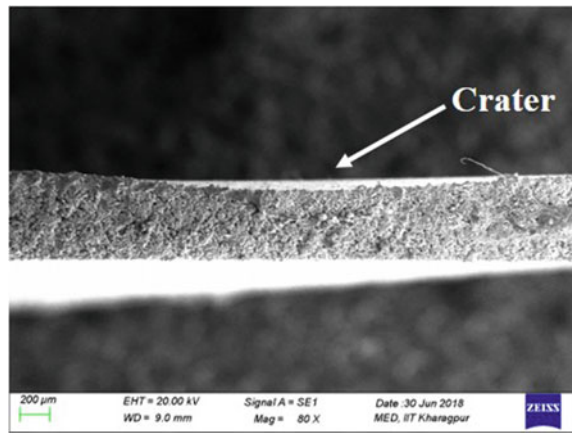
on the output. Thus, higher difference implies a significant influence on the output response. From Fig. 31.8. it can be stated that the order of significant effect on the output is as follows: standoff distance > applied voltage > electrolyte concentration. This is possible because an increase in standoff distance above the threshold value causes the jet to flare out. Flaring of jet increases the effective area of machining, and hence, increases the overall dimension of the machined crater.

31.5 Conclusions

In the present study, electro jet drilling has been successfully used to machine crater of the desired dimension. Applied voltage, concentration of NaCl in the electrolyte and standoff distance was varied to study the change in mass removal rate, roundness error and mean diameter-to-height ratio of the machined crater. The mass removal rate was found to increase with an increase in applied voltage and electrolyte concentration, while the increase in standoff distance was found to cause a decrease in the mass removal rate. The roundness error of the top of the crater was found to increase

with the applied voltage and the standoff distance, while the increase in electrolyte concentration was found to cause a decrease in the roundness error. The mean diameter-to-height ratio of the crater was found to increase with the increase in the electrolyte concentration and the standoff distance, while the increase in applied voltage was found to cause a decrease in the mean diameter-to-height ratio. A confirmation test was performed to obtain the desired crater dimension. It was observed that the optimal combination of process parameters (i.e., applied voltage = 60 V, electrolyte concentration = 0.5 N and standoff distance = 1.5 mm), obtained through grey relational grade analysis, resulted in (a) maximum value of mass removal rate as well as mean diameter-to-height ratio and (b) minimum value of the roundness error of the machined crater. Analysis of average grey relation grade showed that standoff distance has a significant effect on the machining of crater followed by applied voltage and electrolyte concentration.

References

1. Mohan, S., Shan, H.S.: Analysis of hole quality characteristics in the electro jet drilling process. Int. J. Mach. Tools Manuf. **45**, 1706–1716 (2005). https://doi.org/10.1016/j.ijmachtools.2005.03.005
2. Mohan, S., Shan, H.S.: Response surface analysis of electro jet drilled holes. Int. J. Adv. Manuf. Technol. **31**, 520–527 (2006). https://doi.org/10.1007/s00170-005-0196-5
3. Mohan, S., Shan, H.S.: Electro jet drilling using hybrid NNGA approach. Robot. Comput. Integr. Manuf. **23**, 17–24 (2007). https://doi.org/10.1016/j.rcim.2005.08.004
4. Mohan, S., Shan, H.S.: Optimal selection of machining conditions in the electrojet drilling process using hybrid NN-DF-GA approach. Mater. Manuf. Process. **21**, 349–356 (2006). https://doi.org/10.1080/10426910500411561
5. Chen, X.L., Dong, B.Y., Zhang, C.Y., Wu, M., Guo, Z.N.: Jet electrochemical machining of micro dimples with conductive mask. J. Mater. Process. Technol. **257**, 101–111 (2018). https://doi.org/10.1016/j.jmatprotec.2018.02.035
6. Liu, W., Ao, S., Li, Y., LiuZ, Wang Z., Luo, Z., Wang, Z., Song, R.: Jet electrochemical machining of TB6 titanium alloy. Int. J. Adv. Manuf. Technol. **90**, 2397–2409 (2017). https://doi.org/10.1007/s00170-016-9500-9
7. Hua, Zhang, Jiawen, Xu: Modeling and experimental investigation of laser drilling with jet electrochemical machining. Chin. J. Aeronaut. **23**(4), 454–460 (2010)
8. Goel, H., Pandey, P.M.: Performance evaluation of different variants of jet electrochemical micro-drilling process. Proceed. Inst. Mech. Eng. Part B J. Eng. Manuf. **232**, 451–464 (2018). https://doi.org/10.1177/0954405416646689
9. Kozak, J., Rajurkar, K.P., Balkrishna, R.: Study of electrochemical jet machining process. J. Manuf. Sci. Eng. **118**, 490–498 (1996). https://doi.org/10.1115/1.2831058
10. Ming, P., Li, X., Zhang, X., Song, X., Cai, J., Qin, G., Yan, L., Zheng, X.: Study on Kerosene submerged jet electrolytic micromachining. Procedia CIRP **68**, 432–437 (2018). https://doi.org/10.1016/j.procir.2017.12.091
11. Endo, H., Murahashi, T., Marui, E.: Accuracy estimation of drilled holes with small diameter and influence of drill parameter on the machining accuracy when drilling in mild steel sheet. Int. J. Mach. Tools Manuf **47**, 175–181 (2007). https://doi.org/10.1016/j.ijmachtools.2006.02.001
12. Natsu, W., Ooshiro, S., Kunieda, M.: Research on generation of three-dimensional surface with micro-electrolyte jet machining. CIRP J. Manuf. Sci. Technol. **1**, 27–34 (2008). https://doi.org/10.1016/j.cirpj.2008.06.006